WHEEL SLIP CONTROL USING GAIN-SCHEDULED LQ - LPV/LMI ANALYSIS AND EXPERIMENTAL RESULTS

Idar Petersen[†], Tor A. Johansen[*,†], Jens Kalkkuhl[‡] and Jens Lüdemann[‡]

[†]SINTEF Electronics and Cybernetics, N-7465 Trondheim, Norway.
[*]Department of Engineering Cybernetics, Norwegian University of Science and Technology, N-7491 Trondheim, Norway.
[‡]DaimlerChrysler AG, Research and Technology, RIC/AR HPC T728, D-70546 Stuttgart, Germany.

Keywords: Automotive control, gain scheduling, nonlinear systems, robustness, linear matrix inequalities.

Abstract

A wheel slip controller for Anti-lock Brake Systems (ABS) is designed using LQ-optimal control. The controller gain matrices are gain scheduled on the vehicle speed. A parameter dependent Lyapunov function for the nominal linear parameter varying (LPV) closed loop system is found by solving a linear matrix inequality (LMI) problem. This Lyapunov function is used to investigate robustness with respect to uncertainty in the road/tyre friction characteristic. Experimental results from a test vehicle with electromechanical brake actuators and brake-by-wire show that high performance and robustness are achieved.

1 Introduction

Automotive anti-lock brake systems (ABS) controls the slip of each wheel to prevent it from locking such that a high friction is achieved and steerability is maintained. ABS are characterized by robust adaptive behaviour with respect to highly uncertain tyre characteristics and fast changing road surface properties [2, 19, 25]. The introduction of advanced functionality such as ESP (electronic stability program), drive-by-wire and more sophisticated actuators offer both new opportunities and requirements for a higher performance in ABS brakes.

The contribution of the present work is a study of a model-based design of wheel slip control. We consider electromechanical actuators [7, 20] rather than hydraulic actuators. They allow continuous adjustment of the clamping force. The wheel slip dynamics are highly nonlinear and uncertain. Despite this, our control design relies on local linear quadratic regulators using linearization and gain-scheduling. In order to analyze the effects of this simplification, we develop a Lyapunov based stability and robustness analysis. Results from experiments using a test vehicle are also included. The results presented here extend the preliminary results [10, 18], primarily that the stability analysis is more realistic as it is based on a 4th order model rather than a 2nd order model. Also, means to improve the transient performance at low slip are described.

Other contributions to model-based wheel slip control can be found in the literature. The model based approach in [4] applies a search for the optimum brake torque via sliding modes. This approach requires the tyre force, hence, a sliding observer is used to estimate it. Another theoretical approach is presented by [5]. Freeman designs an adaptive Lyapunov based nonlinear wheel slip controller. A similar controller is found in [27] by introducing speed dependence of the Lyapunov function and also including a model of the hydraulic circuit dynamics. Dynamic friction models for the road/tyre characteristics using conventional nonlinear control have been reported in [3, 26]. The use of Sontag's formula is applied in the adaptive control Lyapunov approach in [17]. PID-type approaches to wheel slip control are considered in [8, 12, 22–24]. In contrast, our controller contains no explicit friction model and relies on integral action rather than adaption in order to eliminate steady-state uncertainty. This simplifies the design and may improve the robustness as the friction is difficult to model accurately for a wide range for tyres and surfaces.

2 Wheel slip dynamics

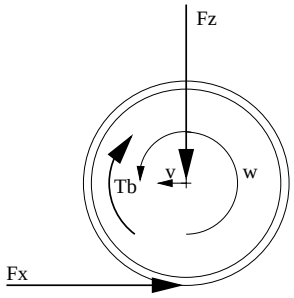

Figure 1: Quarter car forces and torques.

In this section, we review a mathematical model of the wheel slip dynamics, see also [2, 4, 5]. The problem of wheel slip control is best explained by looking at a quarter car model as shown in Figure 1. The model consists of a single wheel attached to a mass m. As the wheel rotates, driven by inertia of the mass m in the direction of the velocity v, a tyre reaction force F_x is generated by the friction between the tyre surface and the road surface. The tyre reaction force will generate a torque that initiates a rolling motion of the wheel causing an angular velocity ω. A brake torque applied to the wheel will act against the spinning of the wheel causing a negative angular acceleration. The equations of motion of the quarter car are

$$m\dot{v} = -F_x \tag{1}$$

$$J\dot{\omega} = r\,F_x - T_b\,\mathrm{sign}(\omega) \tag{2}$$

where v is the horizontal speed at which the car travels, ω is the angular speed of the wheel, F_z is the vertical force, F_x is the tyre friction force, T_b is the brake torque, r is the wheel radius, and J is the wheel inertia. The tyre friction force F_x is given by

$$F_x = F_z \cdot \mu(\lambda, \mu_H, \alpha) \tag{3}$$

where the friction coefficient μ is a nonlinear function of μ_H, the maximal friction between tyre and road, and the slip angle of the wheel, α. The longitudinal slip λ defined by $\lambda = \frac{v-\omega r}{v}$ describes the normalised difference between horizontal speed v and the speed of the wheel perimeter ωr. The slip value of $\lambda = 0$ characterises the free motion of the wheel where no friction

force F_x is exerted. If the slip attains the value $\lambda = 1$, then the wheel is locked. The friction μ can span over a very wide range, but is generally a differentiable function of λ, μ_H and α with the properties $\mu(0, \mu_H, \alpha) = 0$ and $\mu(\lambda, \mu_H, \alpha) > 0$ for $\lambda > 0$. Its typical qualitative dependence on slip λ is shown in Figure 2.

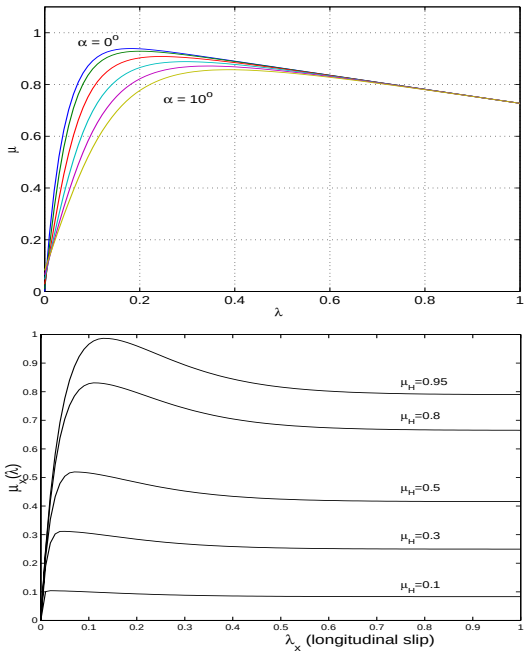

Figure 2: Tyre slip/friction curves $\mu(\lambda, \mu_H, \alpha)$

If the motion of the wheel is extended to two dimensions, then the lateral slip of the tyre must also be considered. The wheel moves with velocity v_x in the longitudinal direction and with a velocity v_y in the lateral direction. In this case, the longitudinal slip $\lambda_x = \frac{v_x - \omega r}{v}$ and the lateral slip $\lambda_y = (1 - \lambda_x) \sin \alpha$ are distinguished as well as the corresponding friction coefficients μ_x and μ_y. The upper part of Figure 2 shows the dependence of the friction coefficient μ_x on the side slip angle α. In the sequel, for simplification purposes unless otherwise stated, the side slip angle will be considered to be zero with $\mu_x = \mu$ and $v_x = v$. Using (1)-(4), for $v > 0$ and $\omega \geq 0$, we get

$$\dot{\lambda} = -\frac{1}{v}\left(\frac{1}{m}(1-\lambda) + \frac{r^2}{J}\right) F_z \mu(\lambda, \mu_H, \alpha) + \frac{1}{v}\frac{r}{J} T_b \quad (4)$$

$$\dot{v} = -\frac{1}{m} F_z \mu(\lambda, \mu_H, \alpha) \quad (5)$$

Note that when $v \to 0$, the open loop slip dynamics (4) becomes infinitely fast with infinite high-frequency gain. This leads to a loss of controllability and the slip controller must be switched off for small v. The following proposition summarizes some useful properties of the closed loop system [18]:

Proposition 1 *Consider the system (4)-(5) with $T_b(t) \geq 0$ for all $t \geq 0$. If $v(0) > 0$ and $\lambda(0) \in [0, 1]$, then $\lambda(t) \in [0, 1]$ and $\dot{v}(t) \leq 0$ for all $t \geq 0$ where $v(t) > 0$.*

3 Control design

The control problem is essentially to control the value of the longitudinal slip λ to a given setpoint λ^* that is either constant or commanded from a higher-level control system such as ESP. The control input is the clamping force F_b that is related to the brake torque as $T_b = k_b F_b$. Integral action or adaptation must be incorporated to remove steady-state errors due to model inaccuracies, in particular the maximum road/tyre friction μ_H. It is essential that the controller maintains a high performance and is robust w.r.t. to any road/tyre friction curve.

The dynamics of the wheel and car body are given by (4) and (5), respectively. Due to large differences in inertia, the speed v will change much more slowly than the slip λ and is therefore a natural candidate for gain scheduling. Thus, for the control design, we consider only (4) and regard v as a slowly time-varying parameter. The control design requires nominal linearized models for design. Let $(\hat{\lambda}, \hat{T}_b)$ be an equilibrium point for (4) defined by the nominal values $\hat{\alpha}$, $\hat{F}_z$ and $\hat{\mu}_H$

$$\hat{T}_b = \left(\frac{J}{mr}(1-\hat{\lambda}) + r\right) \hat{F}_z \mu(\hat{\lambda}, \hat{\mu}_H, \hat{\alpha})$$

The speed-dependent nominal linearized slip dynamics are

$$\dot{\lambda} = \frac{\alpha_1}{v}(\lambda - \hat{\lambda}) + \frac{\beta_1}{v}(T_b - \hat{T}_b) + \text{h.o.t.} \quad (6)$$

where α_1 and β_1 are linearization constants given by

$$\begin{aligned} \alpha_1 &= -\hat{F}_z \left(\frac{1}{m}(1-\hat{\lambda}) + \frac{r^2}{J}\right) \frac{\partial \mu}{\partial \lambda}(\hat{\lambda}, \hat{\mu}_H, \hat{\alpha}) \\ &\quad + \hat{F}_z \frac{1}{m} \mu(\hat{\lambda}, \hat{\mu}_H, \hat{\alpha}) \quad (7) \\ \beta_1 &= \frac{r}{J} \quad (8) \end{aligned}$$

Assuming arbitrary values of α, F_z and μ_H, the wheel slip dynamics (4) can be written in the form

$$\dot{x}_2 = \frac{\phi(x_2)}{v} + \frac{\beta_1}{v}(T_b - T_b^*) \quad (9)$$

where $x_2 = \lambda - \lambda^*$ and λ^* is the desired slip (setpoint). Furthermore, we have defined

$$\begin{aligned} \phi(x_2) &= -\left(\frac{1-\lambda^*-x_2}{m} + \frac{r^2}{J}\right) F_z \mu(x_2 + \lambda^*, \mu_H, \alpha) + \frac{r}{J} T_b^* \\ T_b^* &= \left(\frac{J}{mr}(1-\lambda^*) + r\right) F_z \mu(\lambda^*, \mu_H, \alpha) \end{aligned}$$

It can be seen that (9) has an equilibrium point given by $x_2 = 0$, $T_b = T_b^*$ since $\phi(0) = 0$, and the linearized slip model (6) with a perturbation term written as follows

$$\dot{x}_2 = \frac{\alpha_1}{v} x_2 + \frac{\beta_1}{v}(T_b - T_b^*) + \frac{\epsilon_\mu(x_2)}{v} \quad (10)$$

where $\epsilon_\mu(x_2) = \phi(x_2) - \alpha_1 x_2$. Next, we describe a gain-scheduled LQ approach to wheel slip control design when the actuator dynamics are taken into account, integral action is included and the rate of the clamping force is used as the control input. The latter is introduced partly to simplify the handling of rate constraints in the implementation and partly to get velocity-based gain-scheduled control which has known benefits [15]. The dynamics of the augmented system are

$$\dot{x}_1 = x_2 \quad (11)$$

$$\dot{x}_2 = \frac{\alpha_1}{v} x_2 + \frac{\beta_1}{v}(x_3 - T_b^*) + \frac{1}{v}\epsilon_\mu(x_2) \quad (12)$$

$$\dot{x}_3 = -a(x_3 - T_b^*) + a(x_4 - T_b^*) \quad (13)$$

$$\dot{x}_4 = u \quad (14)$$

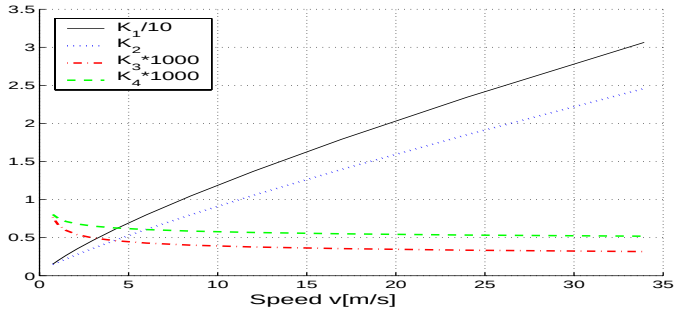

Figure 3: Gain $K(v)$, as a function of v.

The state x_1 is the integrated slip error (giving integral action), x_2 is the slip error, x_3 is the clamping torque produced by the actuator, x_4 is the clamping torque commanded to the actuator and u is its commanded rate of change. The actuator bandwidth is $a = 72$ rad/s. With

$$A(v) = \begin{pmatrix} 0 & 1 & 0 & 0 \\ 0 & \frac{\alpha_1}{v} & \frac{\beta_1}{v} & 0 \\ 0 & 0 & -a & a \\ 0 & 0 & 0 & 0 \end{pmatrix}$$

$$B(v) = \begin{pmatrix} 0 \\ 0 \\ 0 \\ 1 \end{pmatrix}, \quad W(v) = \begin{pmatrix} 0 \\ \frac{1}{v} \\ 0 \\ 0 \end{pmatrix}$$

the system can be written as the following linear parameter-varying (LPV) system with a perturbation:

$$\dot{x} = A(v)(x - x_0) + B(v)u + W(v)\epsilon_\mu(x_2) \qquad (15)$$

where $x_0 = (0, 0, T_b^*, T_b^*)$. The gain-scheduled LQ controller is given in the form $u = -K(v)x$, where the matrix $K(v)$ is computed by solving the following standard linear quadratic optimal control problem

$$J(u, x(t), v) = \int_t^\infty \left(x^T(\tau)Q(v)x(\tau) + Ru^2(\tau)\right) d\tau \qquad (16)$$

We notice that x is known while x_0 is unknown as T_b^* depends on the tyre parameters, vertical load, wheel slip angle, road friction, etc.

The wheel slip approach has been implemented in the ABS system of an experimental test car equipped with electromechanical brakes and a brake-by-wire system. It has the following nominal parameters $m = 450\ kg$, $F_z = 4414\ N$, $r = 0.32\ m$, $J = 1.0\ kg\ m^2$ and the friction model in Figure 2. Assuming $\hat{\lambda} = 0.14$ and the nominal design $\hat{\mu}_H = 0.8$ and $\hat{\alpha} = 0$, we get $\alpha_1 = 10.2$ and $\beta_1 = 0.32$. We notice that since $\alpha_1 > 0$ the chosen operating point is on the unstable part of the friction curve, i.e. to the right of the peak. For the control design, we choose $R = 1$ and $Q(v) = \tilde{Q}v^{3/2}$ with $\tilde{Q}_{1,1} = 8 \cdot 10^6$ and all other elements of $\tilde{Q}$ equal to zero. The choice for $Q(v)$ leads to a gain schedule with reduced gain as $v \to 0$. Reduced gain is useful to avoid instability due to unmodelled dynamics as $v \to 0$, see Figure 3 (K_1 has been reduced by a factor of 10 and K_3 and K_4 increased by a factor 1000 for presentation purposes).

4 Stability and robustness

The control design presented above is based on gain-scheduling and linearized nominal models such that stability should be investigated separately. Moreover, there are numerous uncertain model parameters, the most important being the maximal friction coefficient μ_H, which calls for a robustness analysis. We take a Lyapunov approach based on the closed loop system

$$\dot{x} = (A(v) - B(v)K(v))\, x - A(v)x_0 + W(v)\epsilon_\mu(x_2) \qquad (17)$$

The equilibrium point $x^* = (x_1^*, x_2^*, x_3^*, x_4^*)$ for the closed loop system (17) is now defined by

$$x_1^* = -\frac{K_3(v) + K_4(v)}{K_1(v)} T_b^* \qquad (18)$$

$$x_2^* = 0, \;\; x_3^* = T_b^*, \;\; x_4^* = T_b^* \qquad (19)$$

Defining the error variable $\tilde{x} = x - x^*$, the closed loop system can be written in the following form

$$\dot{\tilde{x}} = (A(v) - B(v)K(v))\tilde{x} + W(v)\epsilon_\mu(\tilde{x}_2) \qquad (20)$$

We note that $\epsilon_\mu(0) = 0$, i.e. it is a vanishing perturbation. In order to analyze the stability and robustness of the closed loop with respect to the uncertain road/tyre friction characteristics, we seek a Lyapunov function for the closed loop system (20). Our approach is first to seek a Lyapunov function that proves uniform exponential stability of origin of the nominal LPV closed loop system

$$\dot{\tilde{x}} = A_0(v)\tilde{x} \qquad (21)$$

with $A_0(v) = A(v) - B(v)K(v)$. The next step is to study if the stability margin provided by this Lyapunov function is sufficient to show robustness with respect to a large class of unknown tyre/road friction characteristics influencing the vanishing perturbation ϵ_μ. We will utilize standard methods for LPV systems, namely a parameter-dependent quadratic Lyapunov-candidate, and formulate the problems in terms of LMIs. Let the Lyapunov function candidate be

$$V(\tilde{x}) = \tilde{x}^T P(v)\tilde{x} \qquad (22)$$

where $P(v) > 0$ is symmetric and specified below.

Proposition 2 *Assume there exist a $\gamma > 0$ and a smooth function $P(v)$ that satisfies for all $v_{max} \geq v \geq v_{min} > 0$*

$$P(v) > 0 \qquad (23)$$

$$\frac{dP}{dv}(v) \geq 0 \qquad (24)$$

$$P(v)A_0(v) + A_0^T(v)P(v) + \gamma P(v) \leq 0 \qquad (25)$$

Then, the origin is a uniformly exponentially stable equilibrium for all trajectories of the nominal closed loop system (21) that satisfies $-\lambda^* \leq x_2(0) \leq 1 - \lambda^*$, $x_3(t) \geq 0$, $x_4(t) \geq 0$ and $v_{max} \geq v(t) \geq v_{min}$ for all $t \geq 0$.

Proof. V is a suitable Lyapunov function candidate since (23) ensures that it is upper and lower bounded by positive definite quadratic functions in $\tilde{x}$ for all $v \geq v_{\min}$. Along trajectories of the nominal closed loop (21), the time-derivative of V is

$$\dot{V} = \tilde{x}^T \left(P(v)A_0(v) + A_0(v)^T P(v)\right) \tilde{x} + \tilde{x}^T \frac{dP(v)}{dv} \tilde{x}\dot{v} \qquad (26)$$

It is known from Proposition 1 that $\dot{v} \leq 0$ during braking such that (24) ensures that the last term in (26) is not positive. Hence, (25) implies that

$$\dot{V} \leq -\gamma \tilde{x}^T P(v) \tilde{x} = -\gamma V \tag{27}$$

It is then a standard result by Corollary 3.4, p. 140, in [16], that the origin is uniformly exponentially stable, i.e. $\tilde{x}(t)$ tends to zero exponentially with rate $\gamma/2$. □

In order to transform these conditions to standard LMI conditions, we introduce a smooth parameterization of $P(v)$ similar to [6] and discretize a suitable interval for the variable v:

$$P(v) = P_0 + P_1 v^{1/2} + P_2 v + P_3 v^{3/2} \tag{28}$$

with symmetric P_0, P_1, P_2 and P_3. The terms depending on v are motivated by the explicit expressions for $P(v)$ solving the algebraic Riccati equation for a similar design based on a 2nd order model [18]. Of course, in the present case, a more complex parameterization may lead to a better Lyapunov function in the sense that it may prove a larger stability margin. Ineq. (23) - (25) now define a standard LMI problem [1] with the objective of maximizing the scalar variable $\gamma > 0$ and when the LMI conditions are imposed at a finite number of values v. A gridding approach is chosen because the parameterization of $P(v)$ is not convex. We have chosen 12 values in the interval $0.75m/s \leq v \leq 33m/s$. This leads to a solution of the LMI conditions (23) - (25) with $\gamma = 26.9$. It follows that the given design makes the equilibrium point $\tilde{x} = 0$ locally exponentially stable when the setpoint is chosen $\lambda^* = 0.14$, even in the presence of uncertainty in the friction curve. The amount of uncertainty may, however, restrict the region of attraction.

Given the $\gamma > 0$ and matrices P_0, P_1, P_2, P_3 that solve the above mentioned LMI-problem, we may examine if the Lyapunov function candidate proves a sufficient stability margin to account for the uncertainty in ϵ_μ. Along the trajectories of the perturbed closed loop (20), the time-derivative of the Lyapunov function V for the nominal closed loop satisfies

$$\dot{V} \leq -\gamma \tilde{x}^T P(v) \tilde{x} + 2\tilde{x}^T P(v) W(v) \epsilon_\mu(\tilde{x}_2) \tag{29}$$

In Figure 4, three figures are shown for $\dot{V}$ as a function of λ; for $v = 0.75, 8.5$ and $25m/s$ respectively. In the left figure, the side slip angle is 15 degrees and zero in the other two figures. In each figure, three curves are shown for $\mu_H (= 0.1, 0.5, 0.9)$. $\tilde{x}_1, \tilde{x}_3$ and $\tilde{x}_4$ are set to their respective equilibrium values. Figure 4 shows that the robust stability requirement (29) is satisfied for all $\tilde{x}_2 \in [-\lambda^*, 1 - \lambda^*]$ for the selected friction curves. Although curves are shown only for $v = 0.75$, 8 and $24m/s$, we have verified that (29) is fulfilled for intermediate values of v, λ and α. Unfortunately, this approach does not allow us to make a rigorous conclusion about anything except local stability since the Lyapunov-function candidate at hand appears to be conservative. However, our analysis indicate the following observations that are in good agreement with our experience from simulations and experiments. First, the robustness margins are most difficult to fulfill at low speed (less than say $5\ m/s$), high μ_H, and large α. This is as excepted, since the uncertainty scales with $1/v$ and at high μ_H and large α, the slip dynamics have the highest degree of open loop instability. Second, largest robustness margins are achieved by placing the setpoint somewhat to the right of the friction curve peak. On the other hand, maximum friction is achieved at the peak value and maximum steerability suggests that the slip is as low as possible. In general, the slip value where the peak value is attained is reduced as μ_H is reduced. Therefore, a reasonable compromise

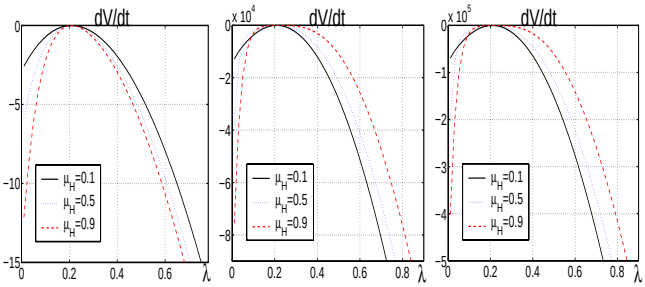

Figure 4: Time derivative of V.

is to let the setpoint be close to the peak value and depend on an estimate of μ_H. This corresponds to generating the nominal model by linearizing near the peak of the nominal friction curve. Note that the only information on the friction curves utilized in the control design, is the slope at the setpoint.

5 Implementation details

Gain scheduling is implemented by switching gain matrices, where the gain matrices are computed for a finite number of operating points (12 velocities logarithmically spaced between 0.75 m/s and 32 m/s). To achieve bumpless transfer, the integrator state x_1 is reset at the switching instants to achieve a control signal without any discontinuities.

The wheel slip λ and the speed v are estimated online using an extended Kalman filter based on wheel speed and acceleration measurements. The slip setpoint, λ^*, is supossed to be provided by a higher level control system. The wheel slip controller is deactivated when the speed is below 1 m/s, and the controller state is reinitialized when the brake pedal is fully released.

The LQ design implemented in the test vehicle differs slightly from the one described above, since it is based on a discretization of the linearized model. This discrete-time model also contains communication delays present in the real-time computer system and explicitly takes into account actuator rate constraints as described in [11].

6 Experimental results and redesign

In this section we describe and discuss three experimental tests, all of which are from braking on dry asphalt, without any steering maneuvers. We only show results for a single front wheel.

The results from the first test are show in Figure 5. The slip setpoint is $\lambda^* = 0.09$ and we note that the regulation is highly accurate and satisfactory. Similar conclusions were made for other road conditions, including ice/snow and wet asphalt [10]. When the speed approaches zero, some variability in the slip emerges. Since the clamping force does not oscillate, we conclude that this is due to sensor noise that is known to increase as the speed goes to zero. However, the initial transient is not satisfactory as the clamping force does not increase fast enough such that the slip is too low and the resulting friction force is too low in the interval $0.2 \leq t \leq 0.7$ leading to increased braking distance. This is due to the significant model inaccuracy in the low-slip region, cf. Figure 2, and a redesign of the slip controller is necessary for this region.

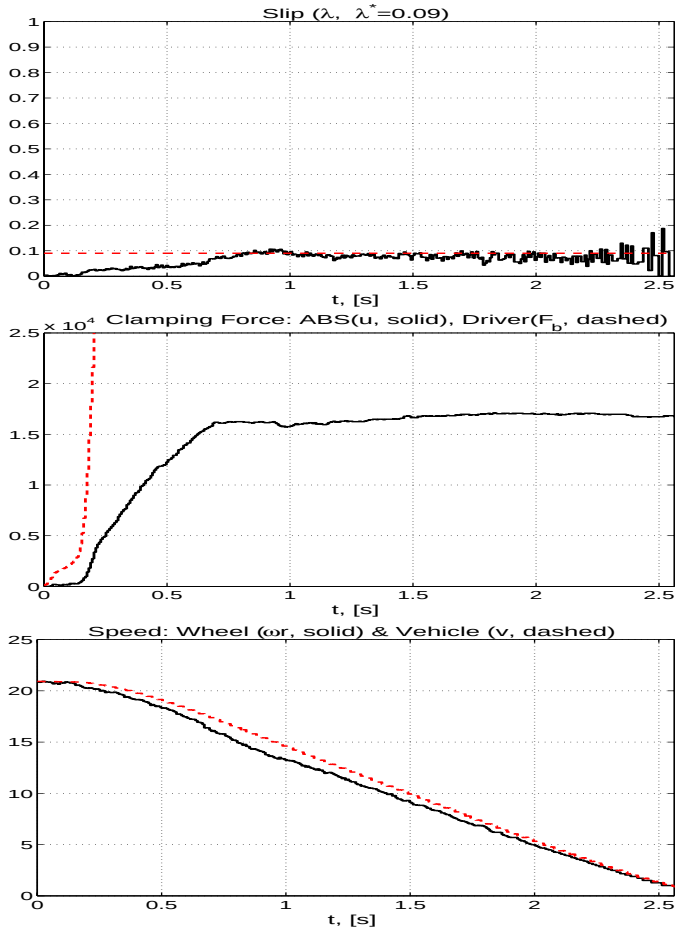

Figure 5: Experimental results with braking on dry asphalt.

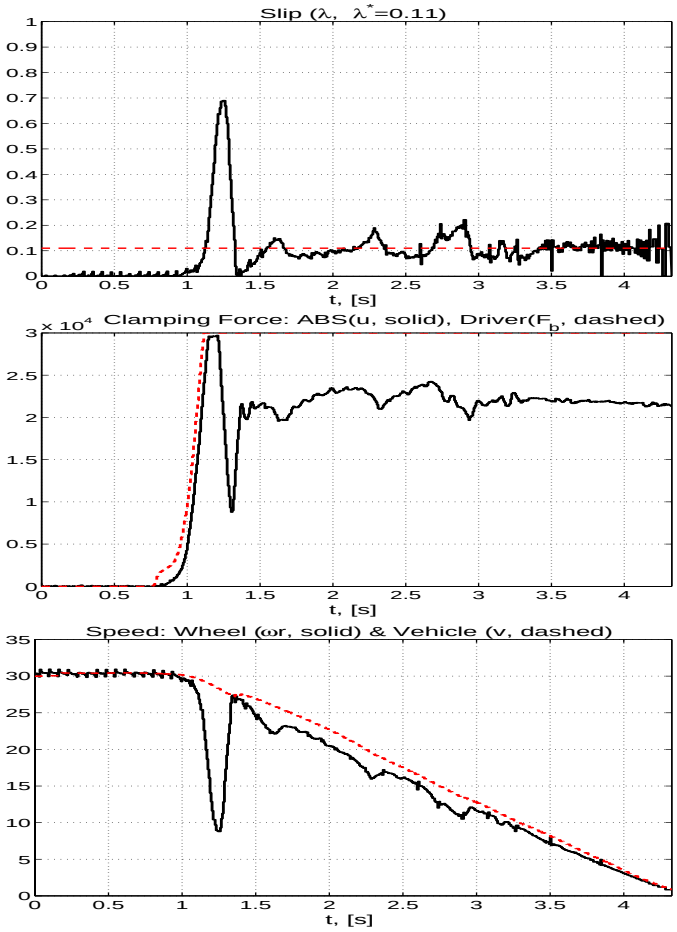

Figure 6: Experimental results with integrator initialization.

We consider two redesign approaches. The first idea is based on the observation that the initial state of the controller will play an important role in the initial transient. In the second test, Figure 6. The slip setpoint is $\lambda^* = 0.11$ and the initial state of the integrator $x_1(0)$ was set to a value that corresponds to the nominal steady-state clamping torque typically required for dry asphalt, using (18). We notice that the initial transient is significantly improved, but with an overshoot that might be reduced by more accurate initialization. Similar ideas were exploited systematically in [13, 14], where a multiple model adaptive control approach with a controller state resetting rule was derived based on an adaptive control Lyapunov function. This allows automatic initialization of the controller state based on an estimate of the current road conditions, and it also provides automatic resetting when the friction coefficient changes abruptly during braking.

The second redesign idea is based on the concept of off-equilibrium linearization and design in gain-scheduled control [9], and is similar to the approach taken in [21]. The idea is to introduce gain-scheduling that is particularly targeted to transient states in addition to conventional gain-scheduling that is targeted to near-equilibrium operation. In the present problem, we essentially switch gain matrices when the slip λ is lower than a given threshold, namely $0.6\lambda^*$. These gain matrices are also designed using LQR based on local linearizations, but the nominal $\hat{\lambda}$ is now on the steep part on the left side of the friction curve, Figure 2, and therefore typically lead to a higher gain than near equilibria. Consequently, the transients are speeded up and the overall performance is improved as shown in the third test, Figure 7. The slip setpoint is $\lambda^* = 0.11$. Again, there is some overshoot, but we believe this can be reduced by fine-tuning of the switching thresholds and the off-equilibrium control design.

7 Conclusions

Using Lyapunov analysis and experimental verification, we have investigated performance and robustness of a model-based nonlinear wheel slip controller for ABS. In order to achieve robustness, the approach does not rely on explicit knowledge of the tyre/road friction curve. Static uncertainty (due to unknown μ_H) is eliminated using integral action, while dynamic uncertainty (due to unknown shape of $\mu(\cdot)$) is handled by a robust design with a sufficient stability margin.

Although a detailed comparison with commercially available off-the-shelf ABS has not been conducted, the present results are encouraging, in particular when taking into account the modest time taken to design, tune and commission this model-based approach. The robustness analysis and redesign based on the experimental experience shows that there are possibilities for further improvement of the control algorithms and tuning.

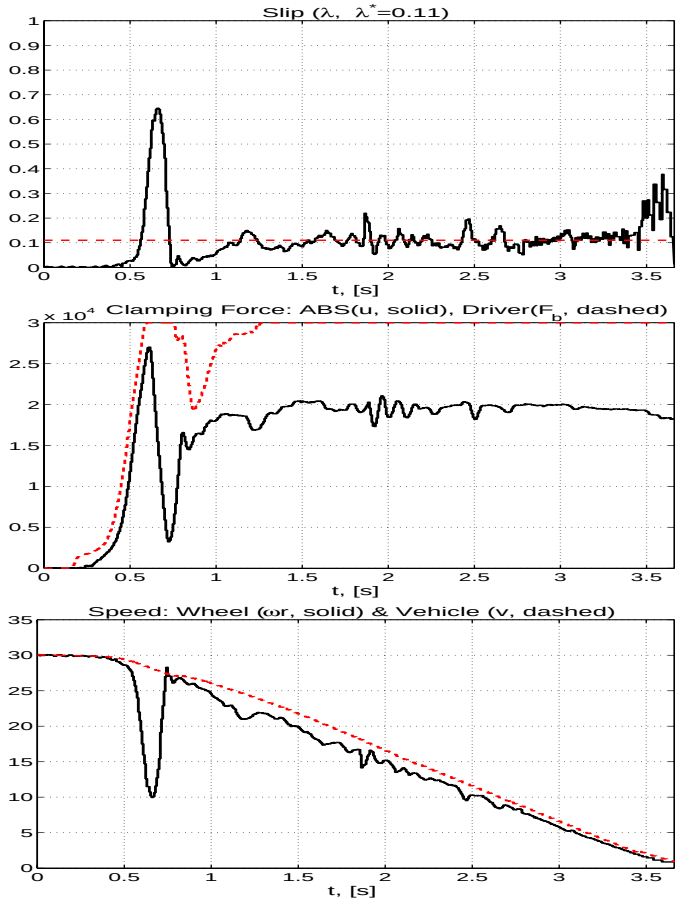

Figure 7: Experimental results with slip/speed scheduling.

Acknowledgements

The work was sponsored by the European Commission under the ESPRIT LTR-project 28104 H_2C. We are grateful to Mr. Lars Imsland for discussion related to LMIs.

References

[1] S. Boyd, V. Balakrishnan, E. Feron, and L. El Ghaoui. Control system analysis and synthesis via linear matrix inequalities. In *Proc. American Control Conference*, pages 2147–2154, 1993.

[2] M. Burckhardt. *Fahrwerktechnik: Radschlupf-Regelsysteme*. Vogel Verlag, Würzburg, 1993.

[3] C. C. de Wit, R. Horowitz, and P.Tsiotras. Model-based observers for Tire/Road contact friction prediction. In H. Nijmeijer and T.I. Fossen, editors, *In New Directions in Nonlinear Observer Design*, pages 23–42. Springer-Verlag, 1999.

[4] S. Drakunov, Ü. Özgüner, P. Dix, and B. Ashrafi. ABS control using optimum search via sliding modes. *IEEE Trans. Control Systems Technology*, 3(1):79–85, 1995.

[5] R. Freeman. Robust slip control for a single wheel. Research Report CCEC 95-0403, University of California, Santa Barbara, 1995.

[6] P. Gahinet, P. Apkarian, and M. Chilali. Affine parameter-dependent Lyapunov function and real parametric uncertainty. *IEEE Trans. Automatic Control*, 41:436–442, 1996.

[7] B. Hedenetz and R. Belschner. Brake-by-wire without mechanical backup using a TTP communication network. In *SAE International Congress and Exhibition, Detroit*, page 981109, 1998.

[8] F. Jiang. *A novel approach to a class of antilock brake problems*. PhD thesis, Cleveland State University, 2000.

[9] T. A. Johansen, K. J. Hunt, P. J. Gawthrop, and H.Fritz. Off-equilibrium linearisation and design of gain scheduled control with application to vehicle speed control. *Control Engineering Practice*, 6:167–180, 1998.

[10] T. A. Johansen, Idar Petersen, Jens Kalkkuhl, and Jens Lüdemann. Gain-scheduled wheel slip control in automotive brake systems. *IEEE Transactions on Control System Technology*, 11, 2003.

[11] T. A. Johansen, Idar Petersen, and Olav Slupphaug. Explicit sub-opitmal linear quadratic regulation with input and state constraints. *Automatica*, 38:1099–1111, 2002.

[12] Cheng Jun. The study of ABS control system with different control methods. In *Proceedings of the 4th International Symposium on Advanced Vehicle Control*, pages 623–628, Nagoja, Japan, 1998.

[13] J. Kalkkuhl, T. A. Johansen, and J. Lüdemann. Improved transient performance of nonlinear adaptive backstepping using estimator resetting based on multiple models. *IEEE Trans. Automatic Control*, 47:136–140, 2002.

[14] J. Kalkkuhl, T. A. Johansen, J. Lüdemann, and A. Queda. Nonlinear adaptive backstepping with estimator resetting using multiple observers. In *Proc. Hybrid Systems, Computation and Control, Rome*, 2001.

[15] I. Kaminer, A. M. Pascoal, P. P. Khargonekar, and E. E. Coleman. A velocity algorithm for the implementation of gain-scheduled controllers. *Automatica*, 31:1185–1191, 1995.

[16] Hassan K. Khalil. *Nonlinear Systems*. Prentice Hall, 1996.

[17] Jens Lüdemann. *Heterogeneous and Hybrid Control with Application in Automotive Systems*. PhD thesis, Glasgow University, 2002.

[18] I. Petersen, T. A. Johansen, J. Kalkkuhl, and J. Lüdemann. Wheel slip control in ABS brakes using gain scheduled constrained LQR. In *European Control Conference*, Porto, 2001.

[19] SAE. Anti-lock brake system review. Technical Report J2246, Society of Automotive Engineers, Warrendale PA, 1992.

[20] R. Schwarz. *Rekonstruktion der Bremskraft Bei Fahrzeugen mit Elektromechanisch Betätigten Radbremsen*. PhD thesis, Institut für Automatisierungstechnik der TU Darmstadt, 1999.

[21] S. Solyom. Synthesis of a Model-based Tire Slip Controller. Technical Report ISRN LUTFD2/TFRT - 3228 - SE, Lund Institute of Technology, Department of Automatic Control, 2002. Licentiate thesis.

[22] S. Solyom and A. Rantzer. ABS control - a design model and control structure. In R. Johansson and A. Rantzer, editors, *Nonlinear and Hybrid Control in Automotive Applications*, pages 85–96. Springer-Verlag, 2002.

[23] S. Taheri and E.H. Law. Slip control braking of an automobile during combined braking and steering manoeuvres. In *Advanced Automotive Technologies*, volume 40, pages 209–227. ASME, 1991.

[24] Y. Wang, T. Schmitt-Hartmann, M. Schinkel, and K. J. Hunt. A new approach to simultanious stabilisation and strong simultanious stabilisation with d stability and its application to abs control systems design. In *European Control Conference*, Porto, 2001.

[25] P. E. Wellstead and N.B.O.L. Pettit. Analysis and redesign of an antilock brake system controller. In *IEE Proceedings of Control Theory Application*, volume 144, pages 413–426. IEE, 1997.

[26] Jingang Yi, Luis Alvarez, Roberto Horowitz, and Carlos Canudas de Wit. Adaptive emergency braking control using a dynamical Tire/Road friction model. In *IEEE Conference on Decision and Control, Sydney*, 2000.

[27] J. S. Yu. A robust adaptive wheel-slip controller for antilock brake system. In *Proceedings of the 36th IEEE CDC*, 1997.